

Preparation and performance study of Ti-10Mo-28Nb-3Zr-yTa alloys for biomedical application

Y. Xu^{a,b}, P. Z. Xia^{a*}, Y. Q. Cai^b, Z. Y. Wei^b, S. T. Zhao^b

^a*School of Metallurgy and Energy, North China University of Science and Technology, Tangshan 063210, Hebei, China*

^b*School of Material Science and Engineering, North China University of Science and Technology, Tangshan 063210, Hebei, China*

Ti-10Mo-28Nb-3Zr-yTa series biomedical β -Ti alloys were theoretically designed using non-biologically toxic Ta as the additive element of Ti-10Mo-28Nb-3Zr alloy by d-electronic theoretical alloy design method, expecting to obtain a lower elastic modulus and higher strength alloy that matches human bones. The microstructure, mechanical properties, corrosion resistance, osteogenic experiment and cytotoxicity of the alloys were tested and analyzed. The results show that the addition of an appropriate amount of Ta will help stabilize the β phase of the Ti-10Mo-28Nb-3Zr alloy, and at the same time can effectively reduce the alloy's elastic modulus. The mechanical properties test shows that Ti-10Mo-28Nb-3Zr-6Ta alloy has the minimum elastic modulus of 27.59 GPa, and the compressive strength is 635 MPa, which meets the requirements of human bone mechanical properties and can meet the mechanical fit of human bone. The corrosion resistance result shows that Ti-10Mo-28Nb-3Zr-6Ta alloy has good corrosion resistance, its self-corrosion current density is $2.726 \times 10^{-6} \text{ A} \cdot \text{cm}^{-2}$, self-corrosion voltage is -188.912 mV, and polarization resistance is $1.639 \times 10^5 \Omega \cdot \text{cm}^{-2}$. The osteogenesis experiment shows that Ti-10Mo-28Nb-3Zr-4Ta alloy has the best bone-promoting effect. Cytotoxicity evaluation experiment shows that the RGR of Ti-10Mo-28Nb-3Zr-yTa alloys were greater than 70% of the negative control group, indicates that the biological properties of the alloy are very reliable.

(Received October 01, 2021; Accepted March 2, 2022)

Keywords: Biological activity, D-electron theory, Medical β -Ti alloys, Mechanical properties, Corrosion resistance

1. Introduction

Ti alloy has high specific strength, low elastic modulus, excellent biocompatibility and corrosion resistance, and has broad application prospects in the field of biomedical materials^[1]. However, the elastic modulus of Ti alloy (80 ~ 110 GPa) is still higher than that of human bone (10 ~ 30 GPa)^[2], and excessive elastic modulus will lead to "stress shielding", which affects the clinical application of Ti alloy implants. The development of Ti alloys in recent years is mainly divided into three stages: The first stage is the stage of α -Ti alloys represented by pure Ti and Ti-6Al-4V^[3]. The second stage is the stage of $\alpha+\beta$ alloys represented by Ti-5Al-2.5Fe and Ti-6Al-7Nb^[3-4]. The third stage is the research stage that includes two types of metastable β type and near β type to develop new Ti alloys with better biocompatibility and lower elastic modulus^[4]. Table 1 is the comparison of mechanical properties of Ti alloys in three stages.

* Corresponding author: 485056053@qq.com

<https://doi.org/10.15251/DJNB.2022.171.301>

Table 1. Mechanical Properties of biomedical Ti alloys^[5].

Preparation method	Alloys	Yield strength / MPa	Ultimate strength / MPa	Area shrinkage / %	Elastic Modulus / GPa
	Pure Ti (grade 1~4)	170~485	240~550	25~30	103
Casting	Ti-6Al-4V (annealed) ^[6]	-	1100~1400	-	112
Powder metallurgy	Ti-6Al-7Nb ^[7]	-	900±14MPa	-	114
Powder Forging	Ti-5Al-2.5Fe	895	1020	35	112
Arc melted	Ti-13Nb-13Zr ^[8]	510	732	59	79~84
lasePowder bed fusion in-situ alloying	Ti-12Mo-6Zr-2Fe (TMZF) ^[9]	900~1031	988~1291	-	74~85
Powder sintering	Ti-15Mo-5Zr-3Al(porous) ^[2]	205MPa	-	-	78
Powder Metallurgy	Ti-35Nb-5Ta-7Zr ^[10]	1055±90	433	-	80
Thermomechanical processing	Ti-29Nb-13Ta-4.6Zr ^[11]	1300	-	-	83
Sintering processing	Ti-24Nb-4Zr-7.9Sn (Ti2448) (aged) ^[12]	580~640	665~705		55

There are nearly 100 new types of medical Ti alloys have been reported in China and abroad. The alloying design ranges from binary to six-component alloys, involving nearly 20 kinds of alloying elements^[13]. In general, the α -phase stable elements (Al, O, N and so on) are very effective for the strengthening of Ti alloy, but they usually increase the elastic modulus of the alloy and reduce the plasticity and toughness of the material. However, Zr, Nb, Mo, Ta and other alloying elements can strengthen the Ti matrix alloys and have little adverse effect on the plasticity and toughness of the alloy, which is beneficial to reduce the elastic modulus of the alloy^[5,13]. Zr improves the strength of Ti alloy; Nb is the β stable element of Ti alloy, and can improve the corrosion resistance, mechanical properties and thermal processing properties of the material; Mo is non-toxic, non-allergic and effective β stabilizer for Ti alloys. Ta is a stable element of β -Ti, which can reduce the transition temperature of α/β phase in the alloy^[14].

Adding high melting point elements such as Mo, Nb, Zr, Ta, to prepare β -Ti alloys have problems such as difficulties in alloy preparation and high smelting costs. Simply changing the amount of alloy addition to conduct experiments will require a lot of experimentation and will produce a lot of waste. The experiment is carried out by simply changing the amount of alloy addition, and the experimental workload is largely a lot of waste. The theoretical composition of Ti alloy can be simulated by d-electron theory, which can greatly reduce the difficulty and amount of experiment and reduce the cost of the experiment. Zhao Lichen et al^[15] designed a metastable β Ti alloy Ti-35Nb-10Zr with low modulus based on d-electronic design theory. Ti-29Nb-13Ta-4.6Zr alloy with low elastic modulus has been designed by Japanese scientists using d-electronic design theory^[16].

In the previous work^[17], we have used the d-electron alloy design theory to conduct the composition design and performance tests for Ti-Mo-Nb-Zr system. The experimental results showed that Ti-10Mo-28Nb-3Zr alloy has the lowest elastic modulus of 43.39 GPa and higher compressive strength of 955 MPa in Ti-Mo-Nb-Zr alloy system. The mechanical properties of the alloy are significantly better than those of the alloy in Table 1. However, the elastic modulus of Ti-10Mo-28Nb-3Zr is still higher than that of human bone. Therefore, Ta element is further introduced to retain more β phase at room temperature in order to further to reduce the elastic modulus of the alloy and realize the mechanical adaptation of human bone. Based on the above findings, Ta with stable β phases structure and no biocompatibility was selected as the alloying component in this experiment. Five Ti-10Mo-28Nb-3Zr-yTa (y= 0, 2, 4, 6, 8 wt%) alloys were designed by d-electron theory, and prepared by powder metallurgy technology. The microstructure, mechanical properties, corrosion resistance, bioactivity and cytotoxicity of Ti alloy were tested and analyzed to provide reference for the preparation of biomedical β -Ti alloy with low elastic

modulus and good biocompatibility.

2. Alloy composition design

The d-electronic alloying design theory originates from the molecular orbital calculation method. The elastic modulus range of Ti-10Mo-28Nb-3Zr-yTa alloy is predicted and controlled by combining Bo (Strength of the covalent bond between alloying elements) and Md (Characterization of d orbital energy, which is related to the radius of metal bonds and the electronegativity of elements). The design process is shown in Fig. 1.

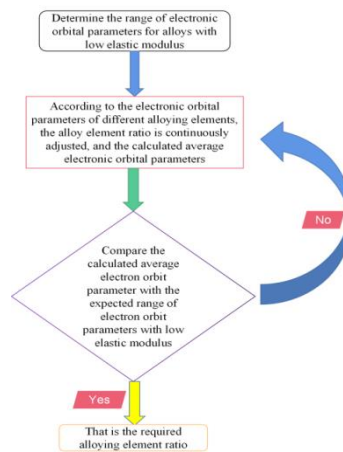


Fig. 1. D-electronic alloying design theory design alloys process.

The Bo , Md values of different alloying elements in β -Ti are shown in Table 2.

Table 2. Bo and Md values of different alloying elements in β -Ti^[18].

	Element	Bo	Md
3d	Ti	2.790	2.447
	V	2.805	1.872
	Cr	2.779	1.478
	Mn	2.723	1.194
	Fe	2.651	0.969
	Cu	2.114	0.567
4d	Zr	3.086	2.934
	Nb	3.099	2.424
	Mo	3.063	1.961
5d	Ta	3.144	2.531
	Al	2.426	2.200

For multivariate Ti-10Mo-28Nb-3Zr-yTa alloys with complex composition, according to the d-electron theory, the average values of Bo and Md of the alloy are defined as follows^[19].

$$Bo = \sum_{i=1}^n x_i(Bo)_i \quad (1)$$

$$Md = \sum_{i=1}^n x_i(Md)_i \quad (2)$$

where, x_i denotes atomic percentage of alloying element i ; $(Md)_i$ denotes Md value of alloying element i ; $(Bo)_i$ denotes Bo value of alloying element i .

For the multivariate β -Ti alloy with complex composition, the larger the Bo value is, the smaller the elastic modulus of the alloy is. And the higher Bo value is conducive to improving the solid solution strengthening effect of the alloy, which can effectively to improve the strength of the alloy^[19]. It is also found that with the increase of Bo value and the decrease of Md value, the phase composition of Ti alloy will change from α phase to $\alpha+\beta$ phase and then to β phase. In order to ensure that the alloy is a β -Ti alloy with low elastic modulus, the Bo value should be as large as possible, and the Md value should be smaller. Chen et al^[20] studied and counted the ranges of Bo and Md of high strength alloys with low elastic modulus were 2.85 ~ 2.88 and 2.43 ~ 2.47. In this paper, the Bo and Md values of Ti-6.28Mo-18.75Nb-2Zr- y Ta alloys are calculated according to the empirical formula for d-electron theory, the results are shown in table 3. The Bo and Md values of Ti-6.28Mo-18.75Nb-2Zr- y Ta alloys range of 2.874~ 2.880 and from 2.423 ~ 2.424, which are in good agreement with the design parameters calculated by Chen Feng and Wang Yu. It is also found that the Bo and Md values of the alloy are higher than those of Ti-10Mo-28Nb-3Zr alloy, and the elastic modulus of the alloy is smaller than that of Ti-10Mo-28Nb-3Zr alloy (This conclusion will be validated in subsequent chapters).

Table 3. Bo , Md values of Ti-10Mo-28Nb-3Zr- y Ta alloys with different Ta content.

Atomic ratio	Mass ratio	Bo	Md
Ti-6.28Mo-18.75Nb-2Zr	Ti-10Mo-28Nb-3Zr	2.871	2.422
Ti-6.25Mo-18.75Nb-2Zr-1Ta	Ti-10Mo-28Nb-3Zr-2Ta	2.874	2.423
Ti-6.25Mo-18.75Nb-2Zr-1.5Ta	Ti-10Mo-28Nb-3Zr-4Ta	2.876	2.423
Ti-6.25Mo-18.75Nb-2Zr-2Ta	Ti-10Mo-28Nb-3Zr-6Ta	2.878	2.424
Ti-6.25Mo-18.75Nb-2Zr-2.5Ta	Ti-10Mo-28Nb-3Zr-8Ta	2.880	2.424

3. Materials and Methods

3.1. Preparation of Ti-10Mo-28Nb-3Zr- y Ta series alloys by powder metallurgy

In this experiment, TiH_2 powder was used to replace high-purity Ti powder because of the low chemical activity of TiH_2 , which reduced the possibility of Ti being oxidized and reduced the oxygen content of the product^[21]. A large number of lattice defects are generated on the surface of fresh Ti produced by direct sintering with TiH_2 as raw material after dehydrogenation, which is beneficial to diffusion and mass transfer, making sintering easier and obtaining higher density^[22-23].

According to the composition ratio of Ti-10Mo-28Nb-3Zr- y Ta ($y = 0, 2, 4, 6, 8$ wt %), commercial TiH_2 ($\leq 74\mu m$), Nb ($\leq 74\mu m$), Mo ($\leq 48\mu m$), Zr ($\leq 48\mu m$) and Ta ($\leq 48\mu m$) powders were milled in a ball miller for 10 hours at a speed of 200 rpm. The blended powders were cold pressed in a mold with dimensions of inner diameter of 10 mm and height of 18 mm under pressure of 800 MPa to prepare green cylindrical compacts and then placed into a tube furnace under protection of argon. The green compacts was heated at a heating rate of $5\text{ }^\circ\text{C}\cdot\text{min}^{-1}$ to $800\text{ }^\circ\text{C}$ for 40 min to dehydrogenate the TiH_2 powders and then heated at a heating rate of $5\text{ }^\circ\text{C}\cdot\text{min}^{-1}$ to $1400\text{ }^\circ\text{C}$ for 2 h to obtain a dense alloy sample.

3.2. Microstructure measurements

Observe the microstructure of the alloys under the OLYMPUS BX51M metallurgical microscope. Phase analysis of Ti-10Mo-28Nb-3Zr- y Ta alloy with D8 ADVANCE small-angle X-ray diffractometer produced by Bruker AXS Company in Germany was carried out. The 2θ range of the test was $20^\circ\sim 80^\circ$, and the diffraction pattern of the alloy sample was obtained.

3.3. Mechanical property measurements

The porosities of alloy sample are obtained by Archimedes drainage method combined with porosity calculation formula. Five Ti alloy's cylinders with diameter of 10 mm and height of

10 mm were selected in each group for room temperature compression test. The stress-strain curve was drawn, and the compressive elastic modulus and compressive strength of the alloy were obtained by taking the average value [24].

3.4. Corrosion resistance tests

The potentiodynamic polarization curves of the samples were obtained by Princeton VersaSTAT 4 electrochemical workstation, and the corrosion resistance of Ti-10Mo-28Nb-3Zr-yTa alloys in human simulated solution is characterized. The human body simulated body fluid formula is shown in Table 4. Three-electrode system is used to draw the Tafel curve. The slope of the polarization curve, self-corrosion current (I_{corr}) and self-corrosion potential (E_{corr}) of the tested sample were obtained. The corrosion resistance R_p is calculated by formula (3).

$$R_p = \frac{\beta_a |\beta_c|}{2.303(\beta_a + |\beta_c|) I_{corr}} \quad (3)$$

where, β_a denotes the slope of anodic polarization, β_c denotes the slope of cathodic polarization, I_{corr} denotes the self - corrosion current ($A \cdot cm^{-2}$).

Table 4. Simulated body fluid formula.

Reagent	Content/ $g \cdot L^{-1}$
NaCl	8.035
NaHCO ₃	0.355
KCl	0.255
K ₂ HPO ₄ ·3H ₂ O	0.231
MgCl ₂ ·6H ₂ O	0.311
HCl	39 ml
CaCl ₂	0.292
Na ₂ SO ₄	0.072
(CH ₂ OH) ₃ CNH ₂	6.118

3.5. Effect of alloying on osteogenic properties of cells

(1) Determination of ALP activity.

Four groups of Ti-10Mo-28Nb-3Zr-yTa ($y = 2,4,6,8$) were selected as the experimental group, and Ti-6Al-4V group was selected as the control group. Five groups of samples were placed in 24-well plate, with 3 multiple holes in each group, and the cell inoculation density was 1×10^4 cells/hole. After 4 and 7 days of culture, the supernatant was collected and centrifuged at $12\,000 \text{ r} \cdot \text{min}^{-1}$ for 15 min. The supernatant was taken and detected by ALP kit. ①Standard curve drawing: The standard protein of $2 \text{ mg} \cdot \text{ml}^{-1}$ was diluted with distilled water to $0.5 \text{ mg} \cdot \text{ml}^{-1}$, and $0.5 \text{ mg} \cdot \text{ml}^{-1}$ standard protein solution of 0, 1, 2, 4, 8, 12, 16, 20 μL was added in 96-well plates in turn; ②Determination of ALP activity in each group: The experimental group was added 20 μL supernatant per well in 96-well plate, and 200 μL buffer solution, matrix solution and chromogenic agent were added. After incubation in dark at $37 \text{ }^\circ\text{C}$ for 30 min, the experimental group was cooled to room temperature. The OD value at 562 nm was measured by SM600 type enzyme-labeled instrument produced by Shanghai Yongchuang Medical Device Co., Ltd., and the content of ALP was calculated according to the standard curve.

Formation of mineralized nodules and detection of calcium concentration.

A bottle of cells with good growth condition was selected. After digestion and centrifugation, the cell density was adjusted to 1×10^4 cells/well by complete medium, and the cell suspension was inoculated into 24-well plate, 1 ml per well. Each group was divided into three multiple holes, a total of five groups. After 24 h cultures in saturated humidity, $37 \text{ }^\circ\text{C}$, 5% CO₂ cell culture box, abandoned the culture medium, respectively, adding five groups of osteogenic induction liquid extracts, each hole 1 ml, every 2 days exchange liquid. The orifice plate was taken

out on the 21st day for dyeing observation. After staining, 500 μl CPC solution was added to each well and incubated at 37 °C for 1 h. After the dyeing part was completely dissolved, 100 μl liquid per well was moved to 96-well plate, and the OD value was measured at 562 nm.

Table 5. Materials used in cytotoxicity test and osteogenic experiment.

Material	Source
L929 mouse fibroblasts	Laboratory of School of Stomatology, North China University of Science and Technology provides
Fetal calf serum	Cegrogen, Germany
PBS buffer	BI, Israel
RPMI1640(Medium)	BI, Israel
CC-K8 Kit	JET, Canada
Double anti-penicillin solution	GIBCO, USA
Trypsin	BI, Israel
Ethyl alcohol	Tansoole, Shanghai
CPC Powder	Tansoole, Shanghai
Vitamin c	Tansoole, Shanghai
Sodium β -glycerophosphate	Tansoole, Shanghai
Alizarin red S dye solution	Tansoole, Shanghai

3.6. Cytotoxicity assays

According to the increase of Ta content in Ti-10Mo-28Nb-3Zr-yTa ($y = 2, 4, 6, 8$), it was divided into four experimental groups (15 circular specimens/groups, 10 mm in diameter and 2 mm in thickness). The negative control group (group E) was 18 ml culture medium containing 10 % FBS. At the same time, the blank control group was established. After sterilization, the specimens were placed in 96-well plates, and the ratio of surface area to volume of extraction liquid was $1.25 \text{ cm}^2 \cdot \text{ml}^{-1}$. All specimens were extracted in RPM1640 medium containing 10 % FBS at 37 °C for 72 h in 5 % CO_2 incubator, and then filtered by 0.22 μm filter membrane. L929 cells in logarithmic growth phase were synchronized with medium containing 0.5 % FBS for 24 h. The old medium was replaced with the extracts of groups A, B, C and D, respectively. The medium containing 10 % FBS was added to group E, and no cells in the blank control group only had complete medium. The plates were cultured in incubators at 37 °C, 5 % CO_2 and saturated humidity. The 96-well plates marked respectively were taken out at 4 p. m. on the 1st, 3rd and 5th day, respectively. The cell morphology was observed under an inverted phase contrast microscope and the images were collected. After collection, the extract was discarded, and 10 μl CCK8 was added to each well. Then the plates were cultured in incubators at 37 °C, 5 % CO_2 and saturated humidity for 24 h, and the plates were taken out every other day. Adjust the wavelength of 490 nm, detect the OD value of each hole, record the results. The relative growth rate (RGR) is the percentage of the ratio of the average OD value of the experimental group to the average OD value of the negative control group. According to GB/T 16886.5-2017/IOS 10993-5: 2009 *Biological evaluation of medical devices Part 5: Cytotoxicity test in vitro*, when RGR decreased to less than 70 % of the negative control group, it has potential cytotoxicity.

4. Results and discussion

4.1. Microstructure characterization

Fig. 2 shows the microstructure of Ti-10Mo-28Nb-3Zr-yTa alloys with Ta content of 0 wt%, 2 wt%, 4 wt%, 6 wt%, and 8 wt%. It can be seen from Fig.2 that the addition of Ta element

will make the acicular martensite in the phase structure of Ti-10Mo-28Nb-3Zr alloy disappear, and the fine β -Ti grains increase significantly, resulting in a large number of defects in the alloying phase structure. When the addition amount of Ta increased from 2 wt% to 6 wt%, the lamellar β -transformed microstructure in the alloying phases gradually decreased, the grain sizes with different sizes became fine and uniform, the number of crystal defects significantly decreased, and the microstructure of the alloying phase became more compact. When the content of Ta element is 6 wt%, the size of lamellar β transformation microstructure is relatively refined and uniform, the microstructure defects are less, and the structure is the most dense. When the content of Ta element increased from 6 wt% to 8 wt%, the lamellar β -transition structure with different sizes appeared again and more defects were found. And, no obvious distinction between α and β phases was found in the alloying phase. The experimental phenomena are in accordance with the rule that a certain amount of Ta element plays a major role in reducing the transition temperature of β phase in multi-component Ti alloys with complex composition, which makes it easier to produce the uniform and fine β phase. However, excessive addition of Ta element will reduce the overall stability of the alloys. In summary, when the additional amount of Ta in Ti-10Mo-28Nb-3Zr-yTa is 6 wt %, it is more likely to form a multi-component Ti alloy with stable β phase.

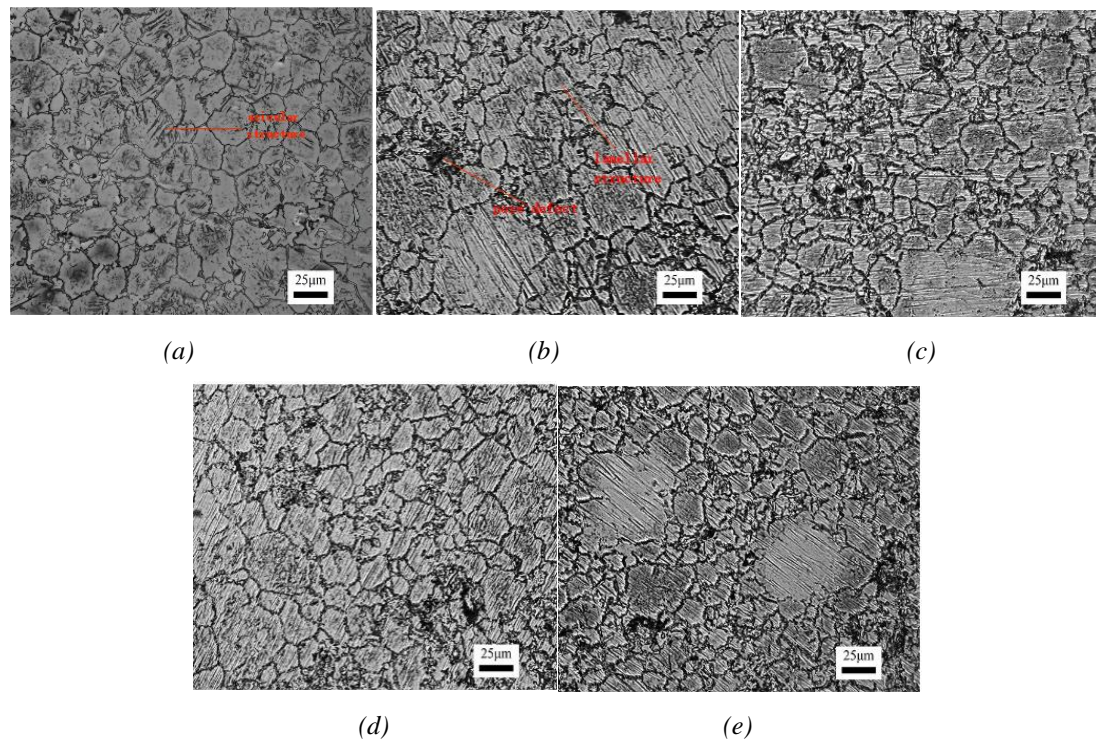


Fig. 2 Microstructures of Ti-10Mo-28Nb-3Zr-yTa alloys with different Ta content
(a) 0 wt%; (b) 2 wt%; (c) 4 wt%; (d) 6 wt%; (e) 8 wt%

Fig. 3 shows the XRD test results of Ti-10Mo-28Nb-3Zr-yTa alloys with Ta content of 0, 2, 4, 6 and 8 wt%. It can be seen from Fig. 3 that the Ti-10Mo-28Nb-3Zr-yTa alloy is mainly composed of β phase. When the content of Ta element increased from 0 to 6 wt%, the intensity of diffraction peaks corresponding to (110), (200) and (211) crystal planes were enhanced, indicating that the crystallization degree of β -Ti crystal structure in the corresponding crystal plane was better and the crystal plane growth was more complete. When the addition amount of Ta increased from 6 to 8 wt%, the intensities of diffraction peaks corresponding to (110), (200) and (211) planes decreased, indicating that the defects in the crystal plane increased, and the β phase decreased, resulting in the decrease of diffraction peaks. When the addition amount of Ta was 6 wt%, the intensities of diffraction peaks corresponding to (110), (200) and (211) crystal planes were the highest, indicating that the crystallization degree of β -Ti crystal structure was the most perfect in the corresponding crystal plane, and the crystal plane growth was the most complete. At this time, the content of β phase in the alloying phase was the most.

When Ta was not added, there was no obvious α phase in the microstructure of the alloy. When the addition amount of Ta increased from 0 to 6 wt%, the α phase in the alloy gradually increased. When the addition amount of Ta was 6 wt%, the diffraction peaks corresponding to the (100) and (330) crystal planes in the alloying phase reached the maximum, and the content of α phase was the largest at this time, but the content of α phase in the alloying phase was significantly lower. In general, the change rule of α phase in the alloying phase is basically the same as that of β phase. It can be speculated that the appearance and change from a small amount of α phase in the alloying phase after adding Ta element may be the secondary α phase produced by the transformation microstructure of β phase.

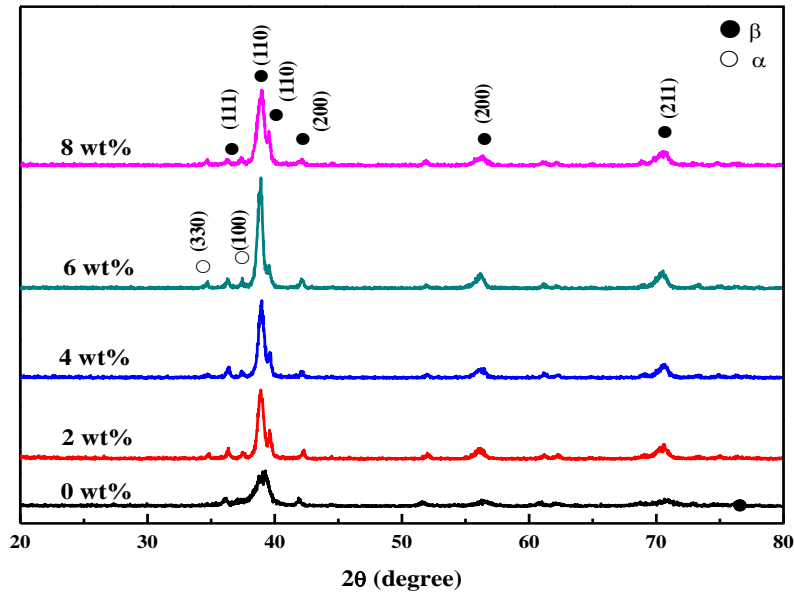


Fig. 3. XRD of Ti-Mo-Nb-Zr-yTa alloys with different Ta content.

4.2. Mechanical properties

Under macroscopic conditions, the increase of porosity in the alloy means that the density decreases, which directly leads to the decrease of the elastic modulus and compressive strength of the alloy. Therefore, in order to study the effect of Ta content on the mechanical properties of Ti-10Mo-28Nb-3Zr-yTa alloy, it is necessary to reduce the effect of alloying porosity on the experiment.

Table 6 shows the porosity of Ti-10Mo-28Nb-3Zr-yTa ($y=0, 2, 4, 6, 8$ wt%) alloys. It can be seen from Table 6 that the porosity differences of the alloy sample remain at about 2% , This showed that the change of Ta content has little effect on the porosity of the sample. It also showed that the change of porosity has little effect on the mechanical properties of samples in this experiment and can be discharged.

Table 6. Porosities of Ti-10Mo-28Nb-3Zr-yTa alloys with different Ta content.

Ta content (wt%)	0%	2%	4%	6%	8%
Porosity	7.27%	7.14%	6.55%	6.82%	8.70%

The two important indexes of mechanical properties of medical Ti alloy are elastic modulus and strength. In clinical application, the strength of medical Ti alloy is required to be larger (the compressive strength of the alloy in the human body ≥ 300 MPa), and the elastic modulus should be as close as possible to the elastic modulus of bone tissue. Fig. 4 is the stress-strain diagram of Ti-10Mo-28Nb-3Zr-yTa alloys with Ta content of 0, 2, 4, 6 and 8 wt%. It

can be seen from the diagram that the stress-strain curves of the five alloys have similar trends. When the stress is small, the alloy has elastic deformation, which is approximately considered to conform to Hooke's law. The stress at the highest point of the curve is compressive strength. The compressive strength of the alloy is obtained by the stress-strain curve. It can be seen from Fig. 4 that with the addition of Ta element, the peak value of the stress-strain curve of the alloy decreases continuously, that is, the compressive strength of the alloy decreases continuously. When Ta content is 0~6 wt%, with the addition of Ta, the peaks value of the stress-strain curve of the alloys decreases slightly, that is, the decrease in the compressive strength of the alloy is small. But when Ta content is 8 wt%, the peak value of the stress-strain curve decreases rapidly, that is, the compressive strength of the alloy decreases greatly^[25].

Fig. 5 shows the compressive elastic modulus and strength of Ti-10Mo-28Nb-3Zr-yTa (y=0, 2, 4, 6, 8 wt%) alloys with Ta content. Fig. 5 further shows the change of compressive strength and elastic modulus with alloy composition. It can be found from Fig. 5 that when the additional amount of Ta is 2 wt%, the compressive strength decreases rapidly from 955 MPa to 660 MPa, which is reduced by about 30%. When the addition of Ta increased to 4 wt%, the compressive strength of the alloy continued to decrease, but the decrease slowed down. When the addition amount of Ta was 6 wt%, the compressive strength of the alloys increased from 570 MPa to 635 MPa. However, when the additional amount of Ta was 8 wt%, the compressive strength of the alloy decreased rapidly again, from 635 MPa to 380 MPa by about 40%. Combined with Fig. 4 and Fig. 5, in order to ensure the compressive strength of the alloy (the compressive strength of the alloy in the human body ≥ 300 MPa), the addition amount of Ta should be controlled at less than 2 wt% or near 6 wt%.

On the other hand, the compressive elastic modulus of the alloy decreases significantly compared with that of the alloy without Ta, which means that the plasticity of the alloy is improved, and the improvement on plasticity can avoid the sudden fracture of Ti alloy due to severe impact. When Ta content is 2 wt%, the compressive elastic modulus of the alloy decreases from 43.5 GPa to 34.3 GPa. When Ta content is 4 wt%, the compressive elastic modulus of the alloy increases slightly compared with the content of 2 wt%. When Ta content is 6 wt%, the compressive elastic modulus of the alloy continues to decrease significantly compared with that of the alloy with 4 wt% Ta, and the minimum compressive elastic modulus is 27.59 GPa. When Ta content is 8 wt%, the compressive elastic modulus of the alloy increases greatly. In conclusion, in order to avoid the 'stress shielding' phenomenon, the alloy should have compressive elastic modulus matching with human bone, so the addition of Ta should be controlled around 6 wt%.

It can be seen from Fig. 5 that when Ta content is 4 wt%, the elastic modulus of the alloy decreases rapidly with the increase in Ta content. The reason for this phenomenon is that with the increase of Ta content, the lamellar β transformation microstructure in the alloying phases begins to refine, and the increase of slip system increases the plasticity of the alloy. The compressive elastic modulus is gradually adjusted with the change of the alloying phase. When Ta content is 6 wt%, the compressive elastic modulus reaches a minimum value of 27.59 GPa, and the compressive strength is 635 MPa. When Ta content is more than 6 wt%, due to the larger flaky β -transformation structure in the alloy phase, the slip surface between the alloy phases decreases, the material tends to be brittle and the defects gradually increase, and its mechanical properties are manifested as an increase in the compressive elastic modulus. The compressive strength drops rapidly.

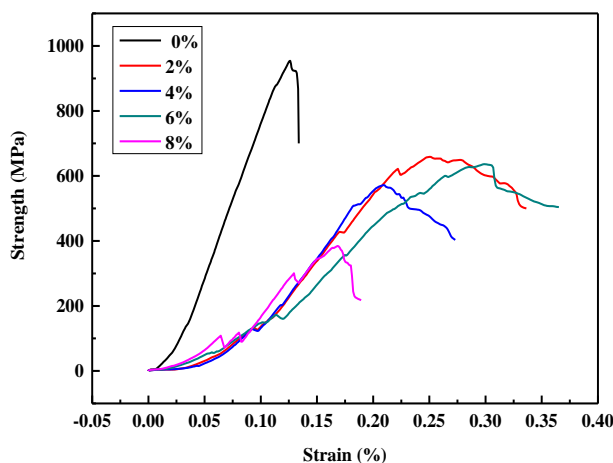


Fig. 4. Stress-strain curve of Ti-10Mo-28Nb-3Zr-yTa alloys with different Ta content.

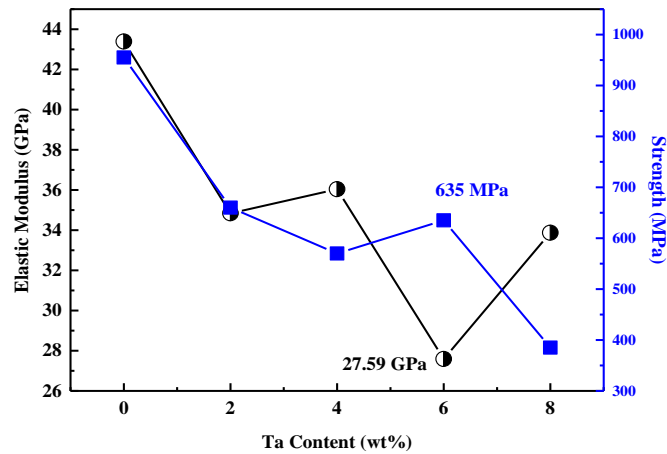


Fig. 5. Elastic Modulus and Strength of Ti-10Mo-28Nb-3Zr-yTa Alloys with Different Ta content.

4.3. Corrosion resistances

The composition of human body fluids is very complex, and medical materials implanted in human body need to maintain basic mechanical properties in this complex composition for a long time. Therefore, for medical materials such as medical Ti alloys that need to be implanted into the human body for a long time, they are research and testing of corrosion behavior in human body fluids are very important. Fig.6 shows the potential polarization curves of Ti-10Mo-28Nb-3Zr-yTa series alloys with Ta content of 0, 2, 4, 6 and 8 wt% in simulated human body fluids. Table 7 shows the electrochemical parameters of Ti-10Mo-28Nb-3Zr-yTa alloys with different Ta content. E_{corr} represents the corrosion tendency towards metal. The larger the value is, the more difficult the metal is to lose electrons or to oxidize, and the smaller the corrosion tendency is. The smaller the value is, the easier the metal loses electrons and is prone to oxidation, so the corrosion tendency is larger. The current density corresponding to the self-corrosion potential E_{corr} is called the self-corrosion current density I_{corr} , which represents the corrosion rate. The greater I_{corr} is, the greater the corrosion rate is. Polarization resistance R_p is obtained by formula (3), which is an important index to judge the corrosion resistance of the alloy. The greater the polarization resistance, the better the corrosion resistance.

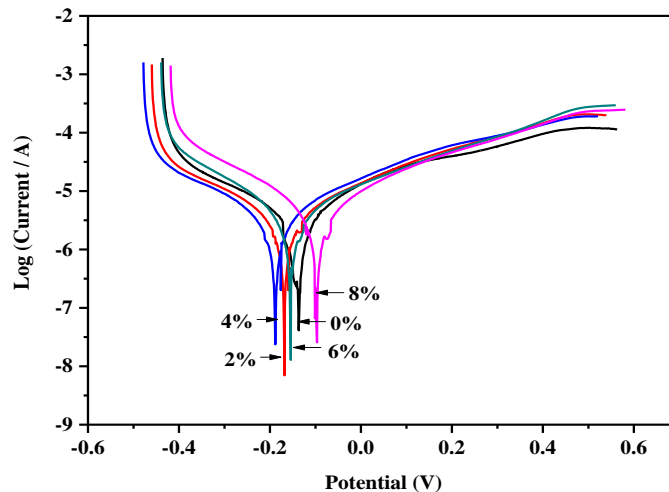


Fig. 6. The potentiodynamic polarization curves of Ti-10Mo-28Nb-3Zr-yTa alloys with different Ta element content.

Table 7. Electrochemical parameters of Ti-10Mo-28Nb-3Zr-yTa alloys with different Ta content.

Ta content	E_{corr} (mV)	$I_{corr} \times 10^{-6}$ ($A \cdot cm^{-2}$)	β_a (mV)	$-\beta_c$ (mV)	$R_p \times 10^5$ ($\Omega \cdot cm^{-2}$)
0 wt%	-145.180	2.962	212.382	208.460	1.542
2 wt%	-172.227	3.024	249.798	210.93	1.642
4 wt%	-188.912	2.726	206.953	204.651	1.639
6 wt%	-149.232	2.282	141.589	144.881	1.363
8 wt%	-94.211	3.791	210.898	210.898	1.208

It can be seen from Fig.6 that alloy samples with different Ta content have similar potentiodynamic polarization curves. In the cathodic polarization region, the current decreases sharply with the increase in potential and is in an unstable state. In the anodic polarization region, with the increase in potential, the current change is small, and the passivation region is formed. Then with the increase of voltage, the current change tend to be stable, and the passivation region is formed. It can obtains from Fig. 6 and Table 11 that the polarization resistance R_p of the alloy increases when the additional amount of Ta increases from 0 wt% to 4 wt%, indicating that the corrosion resistance of the alloy is better. When the Ta content increases from 4 wt% to 8 wt%, the polarization resistance R_p gradually decreases, indicating that the corrosion resistance of the alloy decline. When the addition amount of Ta increased from 2 wt% to 6 wt%, the self-corrosion potential E_{corr} value of the alloy gradually increased, indicating that the alloy was less prone to oxidation and had a smaller corrosion tendency with the increase of Ta content. When the Ta content increases from 2 wt% to 6 wt%, the self-corrosion current density I_{corr} of the alloy gradually decreases, indicating that the corrosion rate of the alloy decreases with the increase of Ta content. Therefore, in general, when the Ta content is 4 wt%, the corrosion resistance of the alloy is relatively excellent, and the self-corrosion current density is $2.726 \times 10^{-6} A \cdot cm^{-2}$, and the self-corrosion voltage is -188.912 mV, which is relatively positive. The polarization resistance of the alloy remained at a large level of $1.639 \times 10^5 \Omega \cdot cm^{-2}$.

4.4. Cell osteogenic properties

In the study of the effects of multi-element Ti alloys with different Ta content of the osteogenic properties of cells, the ALP activity indexes of osteoblasts after 4 and 7 days were measured and statistically analyzed. The results are shown in Table 12. The greater the ALP activity index of osteoblasts, the more obvious the promoting effect of alloy samples of cell osteogenic activity. According to Table 8, the ALP activity of group B was 0.019 ± 0.003 in the five groups of the fourth day. On the seventh day, the ALP activity of group B was the highest in the five groups, which was 0.053 ± 0.016 . This shows that the osteogenic effect of Ti-10Mo-28Nb-3Zr-4Ta group is better than that of the other four groups.

Table 8. ALP activity indexes of osteoblasts measured after different time periods.

Alloying constituent	4d	7d
Ti-10Mo-28Nb-3Zr-2Ta	0.006 ± 0.001	0.014 ± 0.004
Ti-10Mo-28Nb-3Zr-4Ta	0.019 ± 0.003	0.053 ± 0.016
Ti-10Mo-28Nb-3Zr-6Ta	0.011 ± 0.001	0.029 ± 0.003
Ti-10Mo-28Nb-3Zr-8Ta	0.010 ± 0.001	0.025 ± 0.007
Ti-6Al-4V	0.006 ± 0.001	0.008 ± 0.001

The observation of mineralized nodules is shown in Fig. 7. The experimental results show that the formation of mineralized nodules is the most and the staining is the deepest in group B,

indicating that the osteogenesis effect of group B is the best among the five groups of experimental results.

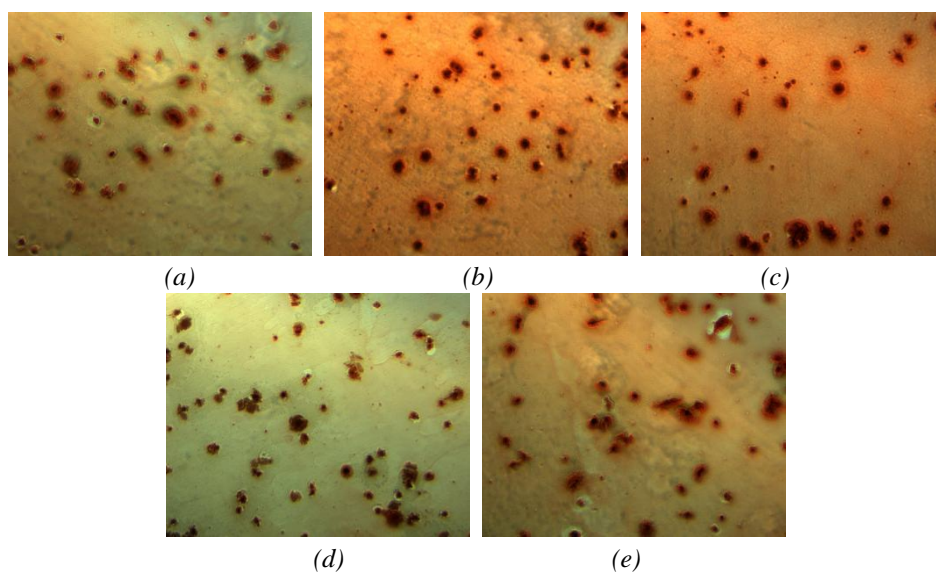


Fig. 7 Observation results of mineralized nodules with different alloying compositions
 (a) Ti-10Mo-28Nb-3Zr-2Ta; (b) Ti-10Mo-28Nb-3Zr-4Ta; (c) Ti-10Mo-28Nb-3Zr-6Ta;
 (d) Ti-10Mo-28Nb-3Zr-8Ta; (e) Ti-6Al-4V

Ca²⁺ concentration tests results are shown in Table 9. Table 9 shows the highest Ca²⁺ concentration of group B compared with the five groups of experimental data. Combined with the observation of mineralized nodules, it can be seen that the osteogenic effect of Ti-10Mo-28Nb-3Zr-4Ta group was significantly better than that of the other four groups.

Table 9. Ca²⁺ concentration detection results.

Alloying constituent	Ca ²⁺ concentration
Ti-10Mo-28Nb-3Zr-2Ta	1.20 ± 0.06
Ti-10Mo-28Nb-3Zr-4Ta	1.32 ± 0.08
Ti-10Mo-28Nb-3Zr-6Ta	1.20 ± 0.02
Ti-10Mo-28Nb-3Zr-8Ta	1.21 ± 0.05
Ti-6Al-4V	1.16 ± 0.08

According to the ALP activity index of osteoblasts, the observation results of mineralized nodules and the detection results of Ca²⁺ concentration, the facilitation effect of Ti-10Mo-28Nb-3Zr-4Ta group was better than that of the other four groups.

4.5. Cytotoxicity test results

In the study of the effect of multi-element Ti alloys with different Ta content of cytotoxicity, cell morphology was observed under the inverted phase contrast microscope after 1, 3 and 5 days of cell culture, as shown in Fig. 8, Fig. 9 and Fig. 10.

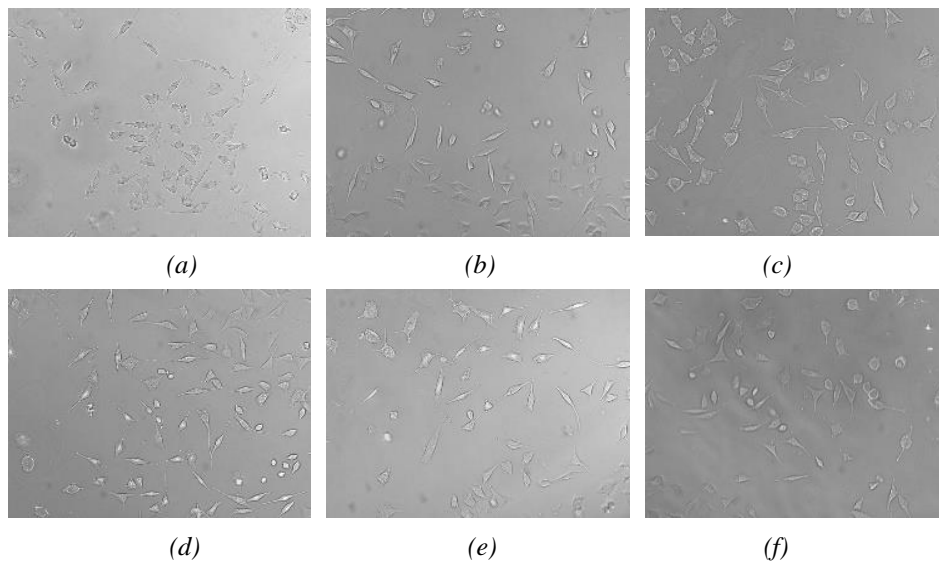


Fig. 8 Cell morphologies in the well plates with different alloying components added after cell culture for 1 day: (a) Ti-10Mo-28Nb-3Zr-2Ta; (b) Ti-10Mo-28Nb-3Zr-4Ta; (c) Ti-10Mo-28Nb-3Zr-6Ta; (d) Ti-10Mo-28Nb-3Zr-8Ta; (e) Blank control group; (f) Negative control group.

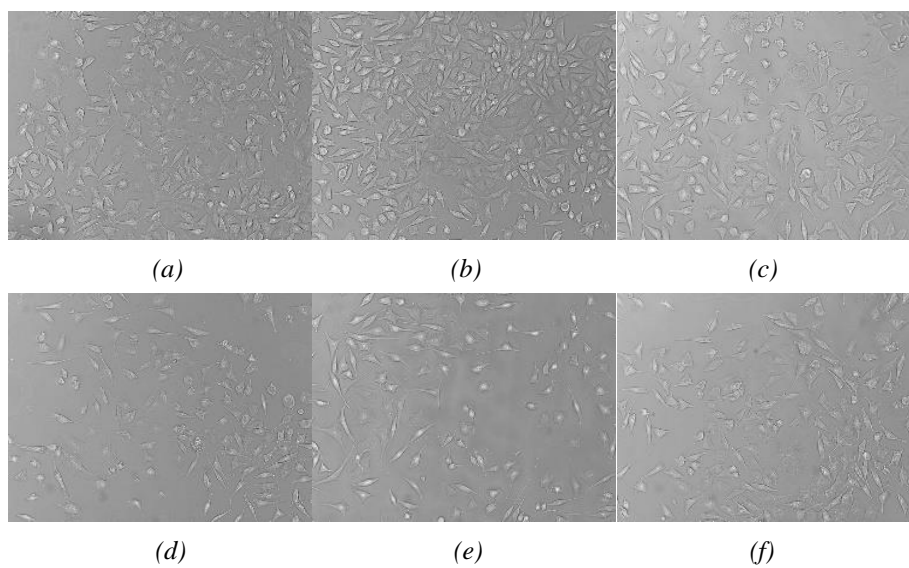


Fig. 9 Cell morphologies in porous plates with different alloying compositions after 3 days culture (a) Ti-10Mo-28Nb-3Zr-2Ta; (b) Ti-10Mo-28Nb-3Zr-4Ta; (c) Ti-10Mo-28Nb-3Zr-6Ta; (d) Ti-10Mo-28Nb-3Zr-8Ta; (e) Blank control group; (f) Negative control group.

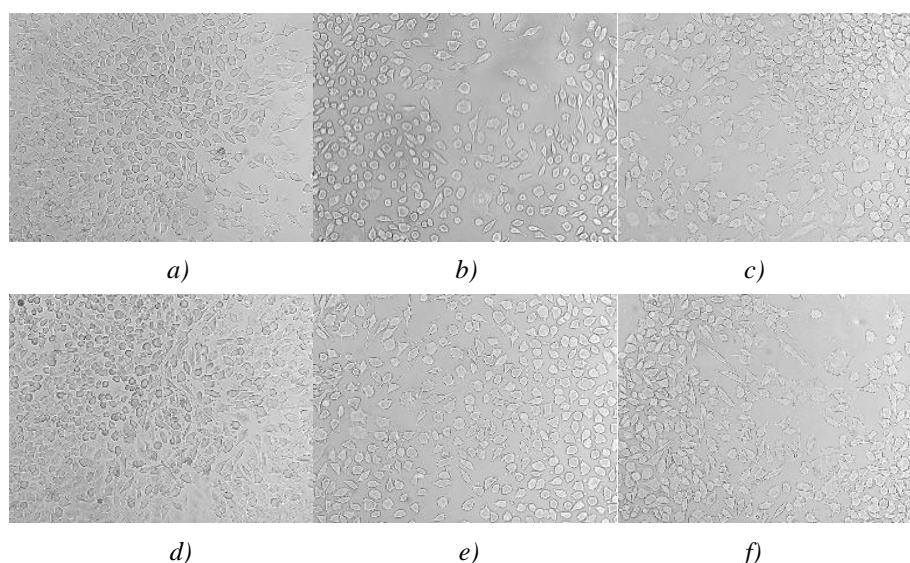


Fig. 10. Cell morphologies in extracts with different alloy components added after cell culture for 5 days (a) Ti-10Mo-28Nb-3Zr-2Ta; (b) Ti-10Mo-28Nb-3Zr-4Ta; (c) Ti-10Mo-28Nb-3Zr-6Ta; (d) Ti-10Mo-28Nb-3Zr-8Ta; (e) Blank control group; (f) Negative control group.

From Fig. 8, Fig. 9 and Fig. 10, it can be seen that the number of cells in the blank control group is lower than that of the other groups when cultured in the same culture period. The number of cells in the four experimental groups is basically the same, and there is no significant difference compared with the negative control group.

CCK8 test results are shown in Table 10. At the same incubation period, the OD value of the blank control group was lower than that of other groups. Except for the blank control group, the OD values of the other four groups increased from the prolongation of culture time.

Table 10. Comparison of OD values of cells in four groups in three time periods.

Group	1d	3d	5d
Ti-10Mo-28Nb-3Zr-2Ta	0.259	0.964	1.183
Ti-10Mo-28Nb-3Zr-4Ta	0.275	0.882	1.172
Ti-10Mo-28Nb-3Zr-6Ta	0.315	0.852	1.170
Ti-10Mo-28Nb-3Zr-8Ta	0.273	0.845	1.225
Negative control group	0.317	0.872	1.400
Blank control group	0.039	0.039	0.213
t factor	F=1253.936		
(Material) Group factors	F=2.528		

The cytotoxicity evaluation is shown in Table 11. The RGR of the four experimental groups of the three periods are all greater than 70% of the negative control group, and the levels of Ti-10Mo-28Nb-3Zr-2Ta and Ti-10Mo-28Nb-3Zr-4Ta were measured on 3 days. RGR was higher than the negative control group, indicating that none of the experimental materials in the 10 groups had potential cytotoxicity. The RGR of the blank control group was all less than 70% of the negative control group.

The comprehensive cell morphologies images, CCK8 test results and cytotoxicity evaluation after different cultures indicate that the newly developed medical Ti-10Mo-28Nb-3Zr-yTa alloying extract has no cytotoxicity to mouse fibroblast L929 cells. The performance is very reliable.

Table 11. Comparison of RGR of cells in four groups in three time periods.

Group	1d	3d	5d
Ti-10Mo-28Nb-3Zr-2Ta	81.7%	110.6%	84.5%
Ti-10Mo-28Nb-3Zr-4Ta	86.8%	101.2%	83.7%
Ti-10Mo-28Nb-3Zr-6Ta	99.3%	97.7%	83.5%
Ti-10Mo-28Nb-3Zr-8Ta	86.0%	96.9%	87.5%
Negative	100%	100%	100%
Blank	12.3%	4.5%	2.8%

5. Conclusion

Ti-10Mo-28Nb-3Zr-yTa ($y = 0, 2, 4, 6$ and 8 wt%) alloys were prepared by powder metallurgy method and sintered at $1400\text{ }^{\circ}\text{C}$ for 2 h. The effects of Ta content on the microstructure, mechanical properties and corrosion resistance of Ti-Mo-Nb-Zr-Ta alloys were investigated. The results show that:

(1) It can be obtained from the analysis of metallurgical and XRD diffraction patterns that with the addition of Ta, the phase structure of Ti-10Mo-28Nb-3Zr-yTa alloy has little difference, and a large number of β -transformation structures begin to appear in the alloy. The β -phase structure of 10Mo-28Nb-3Zr-6Ta alloy is relatively uniform, and the defects in the alloy are the least, and the diffraction peak of β -phase is the strongest, indicating that the Ta content is more conducive to the production of β -phase at 6 wt%.

(2) From the perspective of mechanical properties of biomedical materials, when the Ta content is 6 wt%, Ti-10Mo-28Nb-3Zr-6Ta alloy has the smallest elastic modulus of 27.59 GPa, and the compressive strength is 635 MPa. Finally, the Ti-10Mo-28Nb-3Zr-6Ta alloy has the best mechanical properties and meets the requirements of human bone mechanical properties.

(3) The corrosion resistance of the alloy is related to the microstructure and phase composition of the alloy. When the Ta content is 4 wt%, the Ti-10Mo-28Nb-3Zr-4Ta alloy has a large corrosion voltage of -188.912 mV , a minimum corrosion current density of $2.726 \times 10^{-6}\text{ A}\cdot\text{cm}^{-2}$ and a large passivation resistance of $1.639 \times 10^5\text{ }\Omega\text{ cm}^{-2}$, which has good corrosion resistance.

(4) Based on the effects of five-combination gold samples of the ALP activity of cells, the observation of mineralized nodules and the detection results from Ca^{2+} concentration of five-combination gold samples, it was shown that the osteogenic effect of Ti-10Mo-28Nb-3Zr-4Ta combination gold sample was better than that of the other four groups.

(5) The results of cell morphology and cytotoxicity evaluation show that the new developed medical Ti-10Mo-28Nb-3Zr-yTa alloys have reliable biological properties.

Acknowledgements

We thank North China University of Science and Technology for supporting equipment. Any opinions, findings, conclusions and recommendation expressed in this work are those of authors and do not necessarily reflect the views of the sponsoring agencies.

References

- [1] Hu Jie, Ma Fengcang, Lu Siyao, *Nonferrous Met. Mater. Eng* 40, 1 (2019).
- [2] N. Nomura, T. Kohama, I. H. Oh et al., *Materials Science and Engineering C* 25, 330 (2005); <https://doi.org/10.1016/j.msec.2005.04.001>
- [3] Cai Dandan, Chen Dian, Zhang Gong-Min et al., *China Medical Device Inf* 25, 43 (2019).
- [4] Zhang Yongtao, Liu Hanyuan, Wang Chang et al., *Heat Proces. Techno* 46, 21 (2017).

- [5] Yu Zhentao, Yu Sen, Cheng Jun et al. *J. Met.* 53, 1238 (2017).
- [6] M. T. Jovanović, S. Tadić, S. Zec et al. *Materials & Design* 27, 192 (2006);
<https://doi.org/10.1016/j.matdes.2004.10.017>
- [7] L. Bolzoni, E. M. Ruiz-Navas, E. Gordo, *Journal of the Mechanical Behavior of Biomedical Materials* 67, 110 (2017); <https://doi.org/10.1016/j.jmbbm.2016.12.005>
- [8] C. A. R. P. Baptista, S. G. Schneider, E. B. Taddei et al. *International Journal of Fatigue* 26, 967 (2004); <https://doi.org/10.1016/j.ijfatigue.2004.01.011>
- [9] Ranxi Duan, Sheng Li, Biao Cai et al. *Additive Manufacturing* 37, 101708 (2021);
<https://doi.org/10.1016/j.addma.2020.101708>
- [10] B. Q. Li, X. A. Lu, *J. of Materi Eng and Perform* 28, 5616 (2019);
<https://doi.org/10.1007/s11665-019-04294-7>
- [11] Mitsuo Niinomi, Toshikazu Akahori, Shigeki Katsura et al. *Materials Science and Engineering C* 27, 154 (2007); <https://doi.org/10.1016/j.msec.2006.04.008>
- [12] Shibo Guo, Aimin Chu, Haijiang Wu et al., *Journal of Alloys and Compounds* 597, 211 (2014); <https://doi.org/10.1016/j.jallcom.2014.01.087>
- [13] Ma Xiqun, Yu Zhentao, Niu Jinlong et al., *Appl. Nonferrous Met. Mater. Eng* 39, 26 (2018).
- [14] Li Yongliang. Xiangtan University (2013).
- [15] Wang Xingjuan, Gao Xin, Wang Kuaishe et al., *Hot Working Technol* 42, 14 (2013).
- [16] Ma Rentao, Hao Chuanpu, Wang Qing et al., *Acta Metallurgica Sinica* 46, 1034 (2010);
<https://doi.org/10.3724/SPJ.1037.2010.00039>
- [17] Wei Ziyang, North China University Sci. Technol (2020).
- [18] Yang Yongjian, Sun Wei, Ma Xiumei. *Sci. Technol. Innov. Herald* 16, 10 (2009).
- [19] Wang Guangrong, Gao Qi, Liu Jixiong et al., *Mater. Guide A: Rev* 31, 44 (2017).
- [20] Chen Feng, Wang Yu. *Chinese J. Nonferrous Met* 23, 1560 (2013);
[https://doi.org/10.1016/S1003-6326\(13\)62797-1](https://doi.org/10.1016/S1003-6326(13)62797-1)
- [21] Zhang Jia-Min, Yi Jianhong, Lei Ting et al., *Sci. Technol. Rev* 30, 65 (2012).
- [22] Zhang Ji-Min, Yi Jian-Hong, Gan Guoyou et al., *J. Mater. Eng* 3, 64 (2013).
- [23] Lei Ting, Li Hongmei. *Yunnan Met* 41, 58 (2012).
- [24] Wang Huanhuan, He Shiyu, Xu Ying et al, *Steel Vanadium Titanium* 39, 48 (2018).
- [25] Wu C. D., Fang T. H., Su W. C. et al. *Dig. J. Nanomater. Bios*, 15, 2 (2020).